Synthesis and Characterization of Polyether Adducts of Barium and Strontium Carboxylates and Their Use in the Formation of $MTiO_3$ Films

William A. Wojtczak, Paolina Atanassova, Mark J. Hampden-Smith,* and Eileen Duesler

Department of Chemistry and Center for Micro-Engineered Ceramics, University of New Mexico, Albuquerque, New Mexico 87131

Received May 31, 1996[⊗]

The synthesis, characterization, and reactivity of new polyether adducts of strontium and barium carboxylates of general composition $M(O_2CCF_3)_n(L)$ (M = Ba, L = 15-crown-5, (**1**); M = Ba (**2**), Sr (**3**), respectively, with L = tetraglyme are reported. The compounds were synthesized by reaction of $BaCO_3$ or MH_2 (M = Sr or Ba) with organic acids in the presence of the polyether ligands. These compounds have been characterized by IR and ^{13}C and ^{1}H NMR spectroscopies, elemental analyses, and thermogravimetric analysis. The species $Ba_2(O_2CCF_3)_4$(15-crown-5)$_2$ (**1**) and $[Ba_2(O_2CCF_3)_4(\text{tetraglyme})]_\infty$ (**2**), were also characterized by single-crystal X-ray diffraction. $Ba_2(O_2CCF_3)_4$(15-crown-5)$_2$ (**1**) crystallizes in the orthorhombic space group *Cccm* with cell dimensions of a = 13.949(1) Å, b = 19.376(2) Å, c = 16.029(1) Å, and Z = 8. $[Ba_2(O_2CCF_3)_4(\text{tetraglyme})]_\infty$ (**2**) crystallizes in the monoclinic space group *C2/c* with cell dimensions of a = 12.8673(12) Å, b = 16.6981(13) Å, c = 15.1191(12) Å, β = 99.049(8)°, and Z = 4. Compounds **1**−**3** thermally decompose at high temperatures in the solid state to give MF_2. However, solutions of compounds **1**−**3** dissolved in ethanol with Ti(O-*i*-Pr)$_4$ give crystalline perovskite phase $MTiO_3$ films, or in the case of mixtures of **2** and **3**, $Ba_{1-x}Sr_xTiO_3$ films below 600 °C when spin coated onto silicon substrates and thermally treated. The crystallinity, purity, and elemental composition of the films was determined by glancing angle X-ray diffraction and Auger electron spectroscopy.

Introduction

There is currently a great deal of interest in the preparation of electroceramic powders and films as a result of their realized or potential utility in electronic devices such as multilayer ceramic capacitors (MLCCs) and dynamic random access memories (DRAMs).[1−4] In advanced device structures it is often necessary to achieve greater control over the properties of the electroceramic material such as compositional and phase purity, particle size, and grain size than in other applications. In the case of ferroelectric materials such as $MTiO_3$, the deposition of highly crystalline thin films below 650 °C is necessary for integration into Si-based device structures. Metal−organic routes to electroceramic materials have the potential benefits of better control over composition and lower temperature synthesis over traditional synthetic routes.[5,6] As a result, a great deal of research is being directed at the development of new synthetic routes to perovskite phase materials. There are a number of problems associated with liquid phase metal−organic routes to $BaTiO_3$ films. Metal−organic barium compounds generally exhibit low solubility in organic solvents due to their tendency to oligomerize and they generally have high thermal decomposition temperatures. In addition, thermal decomposition of the metal−organic precursors frequently leads to impurity incorporation into the final material.

Polyether complexes of barium β-diketonates and related derivatives are well-known and have been used as precursors for the chemical vapor deposition (CVD) of Ba-containing materials.[7−16] Fluorinated β-diketonate derivatives have been studied as a result of their lower tendency to dissociate their polyether ligand compared to non-fluorinated derivatives. However, where the deposition pathway involves the thermal decomposition of the β-diketonate ligand, these compounds often lead to the deposition of impure films due to the lack of a suitable mechanism to remove the organic byproducts. In the case of fluorinated derivatives, metal fluorides are often formed as contaminant phases. One solution to this problem is to prepare metal−organic precursors which are designed to undergo reactions which lead to complete elimination of the organic supporting ligands.

In this paper, we report the synthesis and characterization of a number of barium and strontium carboxylate compounds which are soluble in organic solvents with general formula $M(O_2CR)_2L$, and their reactivity toward Ti(O-*i*-Pr)$_4$. These metal carboxylate species incorporate design strategies that have

* Author to whom correspondence should be addressed.

[⊗] Abstract published in *Advance ACS Abstracts,* November 1, 1996.

(1) Brooke, R. J.; Cahn, R. W.; Bever, M. B. *Concise Encyclopedia of Advanced Ceramic Materials*; Pergamon Press: Cambridge, England, 1991.
(2) Chandler, C. D.; Roger, C.; Hampden-Smith, M. J. *Chem. Rev.* **1993**, *93*, 1205.
(3) Jona, F.; Shirane, G. *Ferroelectric Crystals*; Macmillan: New York, 1962.
(4) *IEEE Standard Definitions of Primary Ferroelectric Terms, Std 180−1986*; IEEE: New York, 1986.
(5) Livage, J.; Henry, M.; Jolivet, J. P.; Sanchez, C. *J. Mater. Educ.* **1991**, *13*, 233.
(6) Livage, J.; Henry, M.; Sanchez, C. *Prog. Solid State Chem.* **1988**, *18*, 259.
(7) Malandrino, G.; Fragala, I. L.; Neumayer, D. A.; Stern, C. L.; Hinds, B. J.; Marks, T. J. *J Mater Chem* **1994**, *4*, 1061.
(8) Schulz, D. L.; Hinds, B. J.; Neumayer, D. A.; Stern, C. L.; Marks, T. J. *Chem. Mater.* **1993**, *5*, 1605.
(9) Schulz, D. L.; Hinds, B. J.; Stern, C. L.; Marks, T. J. *Inorg Chem* **1993**, *32*, 249.
(10) Schulz, D. L.; Hinds, B. J.; Neumayer, D. A.; Stern, C. L.; Marks, T. J. *Chem Mater* **1993**, *5*, 1605.
(11) Van der Sluis, P.; Spek, A. L.; Timmer, K.; Meinema, H. A. *Acta Crystallogr., Sect. C* **1990**, *46*, 1741.
(12) Timmer, K.; Spee, C. I. M. A.; Mackor, A.; Meinema, H. A. European Patent 0 405 634 A2, 1991.
(13) Drake, S. R.; Miller, S. A. S.; Hursthouse, M. B.; Malik, K. M. A. *Polyhedron* **1993**, *12*, 1621.
(14) Drake, S. R.; Hursthouse, M. B.; Malik, K. M. A.; Miller, S. A. S. *Inorg. Chem.* **1993**, *32*, 4653.
(15) Drake, S. R.; Miller, S. A. S.; Williams, D. J. *Inorg. Chem.* **1993**, *32*, 3227.
(16) Norman, J. A. T.; Pez, G. P. *J. Chem. Soc., Chem. Commun.* **1991**, 971.

S0020-1669(96)00660-X CCC: $12.00

the potential to solve the problems identified above through the ability to undergo ester elimination and the presence of a multidentate polyether ligand to lower the degree of aggregation. This should also improve solubility in non-aqueous solvents and allow for low temperature thermally-induced ester elimination between the barium carboxylate and titanium alkoxide rather than thermal decomposition. Recent studies in model systems have demonstrated that ester elimination can occur below 100 °C between metal alkoxides and metal carboxylates.[17,18]

Experimental Section

All manipulations were carried out under an atmosphere of dry dinitrogen using standard Schlenk techniques. Hydrocarbon and ethereal solvents were distilled from sodium benzophenone ketyl and stored over 4 Å molecular sieves. The metal starting materials BaH_2, $BaCO_3$, and SrH_2 were obtained from Strem chemical and the carboxylic acids and polyethers, CF_3COOH, 15-crown-5, and tetraglyme, were purchased from Aldrich Chemical Co. All starting materials were used without further purification.

Elemental analyses were performed by Mrs. R. Ju at the Department of Chemistry, University of New Mexico. Nuclear magnetic resonance spectra were recorded on a Bruker AC-250P NMR spectrometer by using the protio impurities of the deuterated solvents as reference for the ^{1}H NMR and the ^{13}C resonance of the solvents as reference for $^{13}C\{^1H\}$ NMR spectroscopy. Infrared data were recorded on a Perkin-Elmer Model 1620 FTIR spectrophotometer. Thermogravimetric analyses were conducted on a Perkin-Elmer Model TGA 7 analyzer. Single-crystal X-ray diffraction data were collected on a Nicolet R3m/v diffractometer. The structures were solved by either the Patterson method or direct methods using SHELXTL Plus and refined by the full-matrix least-squares method. Melting point data were measured on a Thomas-Hoover capillary melting point apparatus.

Synthesis and Characterization. Synthesis of $Ba_2(O_2CCF_3)_4(15\text{-crown-}5)_2$ (1). $BaCO_3$ (0.987 g, 5.0 mmol) and 15-crown-5 (1.0 mL, 5.0 mmol) were stirred in 70 mL of ethanol at −60 °C as CF_3COOH (0.77 mL, 10.0 mmol) was added dropwise. The solution effervesced upon warming to room temperature and became clear after 15 min. Colorless irregular shaped crystals were obtained after placing the solution in a freezer at −20 °C for 2 days. Repeated cycles of concentrating and cooling produced additional crops of crystals; the yield was *ca.* 2.54 g (87%). Anal. Found (calcd for $C_{28}H_{40}O_{18}F_{12}Ba_2$): C, 28.59 (28.78); H, 3.27 (3.45). Thermogravimetric analysis (10 °C/min, in dry air): observed weight loss, 28.9%; expected weight loss, 30.0% (based on BaF_2 formation). ^{1}H NMR (250 MHz, 273K, D_2O): 3.68 ppm, s, crown. $^{13}C\{^1H\}$ NMR (62.9 MHz, 273 K, D_2O, external reference acetone-d_6): 161.0 ppm, q, $^2J_{C-F} = 35.9$ Hz, O_2CCF_3; 114.5 ppm, q, $J_{C-F} = 292.5$ Hz, O_2CCF_3; 68 ppm, s, $C_{10}H_{20}O_5$. IR (KBr, cm^{-1}): 2929 m, 2882 m, 1717 s, 1480 w, 1457 m, 1434 m, 1358 w, 1246 w, 1206 s, 1186 s, 1130 s, 1095 s, 1042 m, 949 m, 864 m, 830 m, 799 w, 718 m. Mp: 260 °C dec (yellow).

Synthesis of $[M_2(O_2CCF_3)_4(\text{tetraglyme})]_\infty$ (M = Ba (2), Sr (3)). MH_2 (Sr, 0.448 g 5.0 mmol; Ba, 1.394 g, 10.0 mmol) and tetraglyme (Sr, 1.1 mL, 5.0 mmol; Ba, 2.2 mL, 10.0 mmol) were stirred in 50 mL of THF (100 mL for M = Ba) at −40 °C as CF_3COOH (Sr, 0.75 mL, 10 mmol; Ba, 1.54 mL, 20.0 mmol) was added dropwise. The MH_2 was rapidly consumed as the solution was warmed to room temperature. The resulting colorless solutions were placed in a freezer at −20 °C for 4 days. Crops of rectangular shaped crystals was isolated by decantation and washed with cold ether; the yield was 1.88 g (88.7%) for M = Sr and 3.92 g (82.7%) for M = Ba. Data for M = Sr follow. Anal. Found (calcd for $C_{18}H_{22}O_{13}F_{12}Sr_2$): C, 25.33 (25.45); H, 2.77 (2.61). Thermogravimetric analysis (10 °C/min, in dry air): observed weight loss, 28.9%; expected weight loss, 29.6% (based on SrF_2 formation). ^{1}H NMR (250 MHz, 273K, acetone-d_6): 3.71−3.55 ppm, m, $-OCH_2CH_2O-$; 3.36 ppm, s, $-OCH_3$. $^{13}C\{^1H\}$ NMR (62.9 MHz, 273 K, acetone-d_6): 163.1 ppm, q, $^2J_{C-F} = 39.6$ Hz, O_2CCF_3; 117.7 ppm, q, $J_{C-F} = 280.5$ Hz, O_2CCF_3; 72.2 ppm, 70.6 ppm, 70.5 ppm, 59.1 ppm, s, $(CH_3OCH_2CH_2OCH_2CH_2)_2O$. IR (KBr, cm^{-1}): 2949 m, 1686 s, 1655 s, 1560 w, 1490 w, 1457 m, 1433 m, 1215 s, 1178 s, 1131 s, 1084 m, 1054 m, 951 m, 855 m, 829 m, 798 m, 728 m, 668 w. Mp: 205 °C dec. Data for M = Ba follow. Anal. Found (calcd for $C_{18}H_{22}O_{13}F_{12}Ba_2$): C, 22.55 (22.78); H, 2.25 (2.34). Thermogravimetric analysis (10 °C/min, in dry air): observed weight loss, 37.5%; expected weight loss, 36.9% (based on BaF_2 formation). ^{1}H NMR (250 MHz, 273K, D_2O): 3.60−3.42 ppm, m, $-OCH_2CH_2O-$; 3.23 ppm, s, $-OCH_3$. $^{13}C\{^1H\}$ NMR (62.9 MHz, 273 K, D_2O, external reference acetone-d_6): 160.8 ppm, q, $^2J_{C-F} = 36.6$ Hz, O_2CCF_3; 114.9 ppm, q, $J_{C-F} = 293.1$ Hz, O_2CCF_3; 69.1 ppm, 67.7 ppm, 67.4 ppm, 56.3 ppm, s, $(CH_3OCH_2CH_2OCH_2CH_2)_2O$. IR (KBr, cm^{-1}): 2940 m, 1689 s, 1654 s, 1558 w, 1542 w, 1492 w, 1457 m, 1436 m, 1352 w, 1208 s, 1181 s, 1131 s, 1088 m, 1057 m, 1017 w, 950 w, 849 w, 828 w, 799 w, 722 w. Mp: 200 °C dec.

X-ray Crystallographic Data. Crystal data for $Ba_2(O_2CCF_3)_4(15\text{-crown-}5)_2$ (1): $C_{28}H_{40}O_{18}F_{12}Ba_2$, orthorhombic, *Cccm*, a =13.949(1) Å, b = 19.376(2) Å, c = 16.029(2) Å, V = 4332.2 (6) Å^3; Z = 8; D_c = 1.790 g cm^{-3}; μ(Mo Kα) = 1.925 mm^{-1}; T = 20 °C, Siemens R3m/v, Mo Kα. Of 9825 data ($3 \le 2\theta \le 55°$), 2591 were independent, and 1636 were observed [$2\sigma(F_o)$]. The structure was solved by the Patterson method. Refinement: the trifluoromethyl groups and 15-crown-5 ligand were rotationally disordered and a detailed description of the disorder model is presented in the supplementary materials. Atoms C2, C4, C5, and O4 of the 15-crown-5 ether are disordered over two positions, and the crown ether itself is disordered around a mirror plane which bisects the Ba, C1, and C6 atoms. This creates a total of four positions for C2, C4, C5, and O4. The positions for these atoms were refined at 0.25 occupancy. The positions for the other crown ether atoms were refined at 0.5 occupancy. It is entirely possible that other positions may exist for the atoms of the 15-crown-5 ether; however, none were obvious from the final difference Fourier map. In addition to the disorder of the 15-crown-5 ligand, the F1, F2, and F3 atoms of the trifluoromethyl groups of the trifluoroacetate ligands are disordered over two positions (53:47). The final model included anisotropic Ba, O6, O7 C7, and C8 atoms, ordered trifluoroacetate ligands (i.e. $-CO_2$), and fixed crown ether positions with all hydrogen atoms in idealized positions, $R(F)$ = 6.28%, $R_w(F)$ = 6.82%, GOF = 1.19, N_o/N_v = 13.1, $\Delta(\rho)$ = 0.70 eÅ^3, $\Delta/\sigma_{(max)}$ = 0.034. SHELXL software was used for all computations (Sheldrick, G. Siemens XRD, Madison, WI). An empirical (ψ-scan) correction was performed. The ratio of the transmission coefficients was 1.14. A decay correction was also applied. Three standard reflections showed an average of 4.03% intensity loss during the data collection.

Crystal data for $[Ba_2(O_2CCF_3)_4(\text{tetraglyme})]_\infty$ (2): $C_{18}H_{22}O_{13}F_{12}Ba_2$, monoclinic, *C*2/*c*, a =12.867(1) Å, b = 16.698(1) Å, c = 15.119(1) Å, β = 98.487 (8)°, V = 3213.9 (5) Å^3; Z = 4; D_c = 1.961 g cm^{-3}; μ(Mo Kα) = 2.559 mm^{-1}; T = 20 °C, Siemens R3m/v, Mo Kα. Of 7578 data ($3 \le 2\theta \le 55°$), 3699 were independent, and 2456 were observed [$2\sigma(F_o)$]. The structure was solved by the Patterson method. Refinement: the trifluoromethyl groups of the acetate ligands were rotationally disordered over two and three sites. The disorder model and information on the site occupancies are presented in the supplementary material. In the final model all non-hydrogen atoms except for the disordered fluorine atoms were refined anisotropically with all hydrogen atoms in idealized positions (riding model) with isotropic displacement parameters set at 1.25U_{equiv} of the corresponding carbon atom, $R(F)$ = 4.22%, $R_w(F)$ = 4.11%, GOF = 0.94, N_o/N_v = 12:1, $\Delta(\rho)$ = 0.77 eÅ^3, $\Delta/\sigma_{(max)}$ = 0.002. SHELXL software was used for all computations (Sheldrick, G. Siemens XRD, Madison, WI). An empirical (ψ-scan) correction was performed. The ratio of the transmission coefficients was 1.21. A decay correction was also applied. Three standard reflections showed an average of 10.65% intensity loss during the data collection.

Film Deposition. The barium, strontium, and barium−strontium titanate thin films were prepared by spin coating silicon or platinum−silicon substrates under a nitrogen atmosphere with ethanol solutions of titanium isopropoxide and the polyether metal carboxylate compounds $[M_2(O_2CCF_3)_4(\text{tetraglyme})]_\infty$ (M = Sr, 0.142 g, 0.167 mmol; Ba, 0.156 g, 0.167 mmol; M = $Ba_{0.7}Sr_{0.3}$, 0.111 g, 0.234 mmol (Ba); 0.0425 g, 0.100 mmol (Sr)) and $Ba_2(O_2CCF_3)_4(15\text{-crown-}5)_2$ (0.196 g,

(17) Caruso, J.; Hampden-Smith, M. J.; Rhiengold, A. L.; Yap, G. *J. Chem. Soc., Chem. Commun* **1995**, 157.
(18) Caruso, J.; Schwertfeger, F.; Roger, C.; Hampden-Smith, M. J.; Rheingold, A. L.; Yap, G. *Inorg. Chem.* **1995**, *34*, 449.

0.167 mmol). The carboxylate compounds were placed in 10 mL Schlenk tubes, and 5 mL of dry ethanol was added to each by syringe. After a few minutes of stirring, the compounds dissolved to give clear solutions. $Ti(i\text{-}OPr)_4$ (0.10 mL, 0.336 mmol) was then added dropwise to each solution to produce a solution composition with a 1:1 M(Sr, Ba):Ti ratio.

The substrates were cleaned prior to use by rinsing them with both acetone and ethanol followed by drying in a oven at 100 °C. Just prior to the spin coating experiments, 1 mL aliquots of the precursor solutions were transferred from Schlenk tubes to 1 mL disposable syringes. These solutions were then deposited dropwise under a nitrogen flow on spinning substrates (3000 rpm, 45 s, approximately 10 drops). The films were annealed in air at 350 °C for 10 min between each deposition. Following the last deposition, the $[M_2(O_2CCF_3)_4(\text{tetraglyme})]_\infty$ (M = Sr, Ba, $Ba_{0.7}Sr_{0.3}$) films were split in half and each one of the halves annealed for 3 h at 575 °C so that both the amorphous (350 °C) and crystalline (575 °C) pieces were of common origin. Separately, films of $Ba_2(O_2CCF_3)_4(15\text{-crown-}5)_2$ were annealed at 350, 450, 550, and 650 °C.

Film Characterization. To evaluate the crystallization process and stoichiometry of the thin films, Glancing Angle X-ray Diffraction (Siemens D5000), Scanning Electron Microscopy (Hitachi 800) and Auger Electron Spectroscopy measurements were conducted. Auger Electron Spectroscopy (AES) data were collected with cylindrical mirror analyzer (PHI 10−155), with an electron beam energy of 3 keV, at a base pressure of 10^{-9} Torr. The Auger peaks of C (KLL) at 271 eV, O (KLL) at 516 eV, Ti (LMM) at 388 eV, Ba (MNN) at 590 eV, F (KLL) at 655 eV, and Sr (LMM) at 1652 eV were used for estimation of the composition and stoichiometry of the samples. An Ar^+ ion gun with ion beam current intensity of 10 μA/cm^2 at 1 keV beam energy and 4×10^{-5} Torr pressure was applied for removing the surface impurities and for depth profiling of the films.

Estimation of the elemental composition by AES was based on the experimental sensitivity factors. Experimental sensitivity factors were obtained from Auger spectra of standard stoichiometric compounds of the elements of interest—$BaTiO_3$, $SrTiO_3$, $BaCO_3$, BaF_2, and TiO_2. At a fixed sensitivity factor for oxygen of $S_0 = 0.5$ derived from the experimental data for stoichiometric compounds, the following relative sensitivity factors were obtained and applied: $S_C = 0.2$, $S_F = 0.47$, $S_{Ba} = 0.39$, $S_{Sr} = 0.054$, $S_{Ti} = 0.33$ (for the above mentioned Auger peaks). This approach proved to be much more accurate compared to application of handbook sensitivity factors.[19] The fluorine composition was estimated taking into account the overlapping of the F(KLL) peak at 655 eV with the low-intensity peak of Ba at the same position based on the relative intensity of this peak in high-purity $BaTiO_3$ and $BaCO_3$.

Results and Discussion

The species $M(O_2CCF_3)_m(L)$, where L = tetraglyme and 15-crown-5, were prepared in high yield by reaction of $BaCO_3$ or BaH_2 with the free acids in the presence of the polyether ligands. The reactions are facile as evidenced by the rapid effervescence of the solutions upon addition of the acids to the metal starting materials. The presence of the polyether ligand during formation of the barium carboxylate is important in some instances for coordination of this ligand to the barium center. We have found that some polyether ligands (e.g. 15-crown-5) do not bind to preformed barium carboxylates (e.g. $Ba(O_2CCH_3)_2$) when dissolved in solvent (water).[20] The fluorinated carboxylate, trifluoroacetate, was chosen because it was expected that the presence of the fluorine atoms might enhance volatility increase solubility and, through an inductive effect, keep the polyether bonded to the metal center. The trifluoroacetate compounds **1**−**3** are soluble in coordinating solvents such as THF and alcohols but only sparingly soluble in hydrocarbon solvents such as toluene.

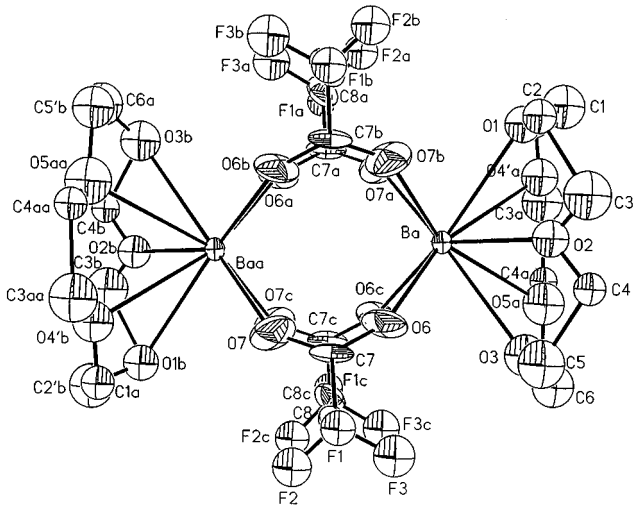

Figure 1. ORTEP plot of the solid-state molecular structure of $Ba_2(O_2CCF_3)_4(15\text{-crown-}5)_2$ (**1**). Hydrogen atoms have been omitted for clarity and only one orientation of the disordered crown ether and fluorine atoms is shown.

Two examples have been structurally characterized in the solid state by single-crystal X-ray diffraction, $Ba_2(O_2CCF_3)_4(15\text{-crown-}5)_2$ (**1**) (Figure 1), and $[Ba_2(O_2CCF_3)_4(\text{tetraglyme})]_\infty$ (**2**) (Figure 2). Important crystallographic parameters are provided in Table 1 and atomic coordinates and relevant bond distances and angles are reported in Tables 2 and 3.

The species $Ba_2(O_2CCF_3)_4(15\text{-crown-}5)_2$ is dinuclear with bridging rather than chelating carboxylate ligands and with the barium atom on one face of the 15-crown-5 ligand. This side-on bonding of the 15-crown-5 ether most certainly arises from the mismatch in size of metal to the crown cavity. The Ba^{2+} ionic diameter is 2.86 Å, whereas the "hole sizes" for the 18-crown-6 and 15-crown-5 ethers have a range of 2.6−3.2 and 1.7−2.2 Å, respectively.[21] Clearly, the barium atom is too large to reside at the center of a 15-crown-5 ring. The Ba−O bond distances can be compared to those of the related compound $Ba(O_2CC\text{-}t\text{-}Bu)_2(18\text{-crown-}6)$ in which the Ba sits in the center of an 18-crown-6 ring with chelating pivalate ligands perpendicular to this coordination plane.[22] The average $Ba-O_{carboxylate}$ bond distance of 2.644[12] Å in **1** is significantly shorter than the average $Ba-O_{carboxylate}$ bond distance of 2.834[18] Å in $Ba(O_2CC\text{-}t\text{-}Bu)_2(18\text{-crown-}6)$.[22] Concomitantly, the O−C−O angle becomes more obtuse (by 7.5°) upon moving from the chelating pivalate ligand to the bridging trifluoroacetate ligand. The lengthening of the $Ba-O_{carboxylate}$ bond distance for a chelating carboxylate ligand is probably associated with keeping the O−C−O angle from becoming too acute (<120°). A shortening of the $Ba-O_{carboxylate}$ bond distances in the trifluoroacetate compound may also arise from the better match between the trifluoroacetate ligand and the barium center on the hard and soft acid−base scale. The $Ba-O_{ether}$ bond distances vary over a wide range of 2.910(34)−2.972(22) Å. The Ba−O4′ and Ba−O5 bond distances are longer than the others by 0.17 and 0.22 Å, respectively. This would suggest asymmetry in the bonding of the 15-crown-5 ether to the barium atom, however; the large esd's of the bond distances of **1** and the severe disorder in the crown ether ligand preclude any definitive statement on the anomalies in the $Ba-O_{ether}$ bond distances.

The species $[Ba_2(O_2CCF_3)_4(\text{tetraglyme})]_\infty$ (**2**) exists as infinite chains in the solid state in which both the carboxylate and

(19) Briggs, D.; Seah, M. P. *Auger and Electron Spectroscopy*; Wiley: New York, 1992; Vol. 1.
(20) Wojtczak, W. A.; Archer, L.; Atanassova, P.; Duesler, E.; Hampden-Smith, M. J. Unpublished results, 1996.
(21) Greenwood, N. N.; Earnshaw, A. In *Chemistry of the Elements*, 1st ed.; Pergamon Press: Oxford, England, 1984.
(22) Rheingold, A. L.; White, C. B.; Haggerty, B. S.; Kirlin, P.; Gardiner, R. A. *Acta Cryst.* **1993**, *C49*, 808.

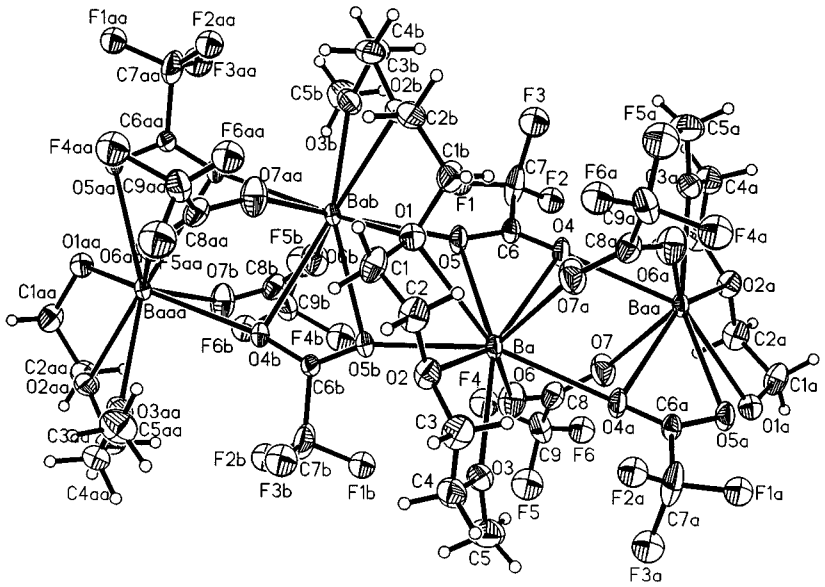

Figure 2. ORTEP plot of the solid-state molecular structure of $[Ba_2(O_2CCF_3)_4(tetraglyme)]_\infty$ (**2**). Hydrogen atoms have been omitted for clarity, and only one orientation of the disordered fluorine atoms is shown.

Table 1. Summary of Crystal Data for $Ba_2(O_2CCF_3)_4(15\text{-crown-}5)_2$ (**1**) and $[Ba_2(O_2CCF_3)_4(tetraglyme)]_\infty$ (**2**)

	$Ba_2(O_2CCF_3)_4$-(15-crown-5)$_2$ (**1**)	$[Ba_2(O_2CCF_3)_4$-(tetraglyme)$]_\infty$ (**2**)
molecular formula	$C_{28}H_{40}Ba_2F_{12}O_{18}$	$C_{18}H_{22}Ba_2F_{12}O_{13}$
fw	1167.2	949.0
a (Å)	13.949(1)	12.867(1)
b (Å)	19.376(2)	16.698(1)
c (Å)	16.029(1)	15.119(1)
β (deg)		98.49(1)
space group	*Cccm* (No. 66)	*C*2/*c* (No. 15)
T (K)	293	293
ρ_{calcd} (g/cm^{-3})	1.790	1.961
λ(Å)	0.710 73	0.710 73
Z	8	4
V (Å^3)	4332.2(6)	3213.9(2)
μ (mm^{-1})	1.925	2.559
R (%)[a]	6.28	4.22
R_w (%)[b]	5.99	4.04

[a] $R = \sum\Delta F/\sum F_o$. [b] $R_w = \sum w^{1/2}\Delta F/\sum w^{1/2}F_o$; $w^{-1} = \sigma^2(F) + 0.0005F^2$.

Table 2. Relevant Bond Lengths (Å) and Angles (deg) for $Ba_2(O_2CCF_3)_4(15\text{-crown-}5)_2$ (**1**)[a]

Bond Distances			
Ba−O1	2.955(22)	Ba−O2	2.972(22)
Ba−O3	2.925(31)	Ba−O4	2.910(34)
Ba···Ba[a]	4.735(1)	Ba−O4′	3.143(69)
Ba−O6	2.652(11)	Ba−O5	3.191(39)
		Ba−O7a	2.635(14)
Bond Angles			
O6−Ba−O7a	123.2(4)	O6−Ba−O6c	78.1(5)
O6−Ba−O7b	75.6(4)	O7−Baa−O7c	78.4(7)
O6−C7−O7	131.3(13)		

[a] Primed atoms denote an alternate disorder position for unprimed atoms.

tetraglyme ligands bridge the barium centers. The barium atoms are arranged in a zigzag fashion within the chains. The compound contains carboxylate ligands that chelate to one barium center (zig) while bridging between two other barium centers (zags) and others that bridge only between two barium centers (zag-to-zig). The tetraglyme ligand bridges between two barium centers (zig-to-zag) through its center oxygen atom (O1). The bridging and chelating carboxylate ligand has average bridging and chelating $Ba-O_{carboxylate}$ bond distances of 2.758[21] and 2.904[70] Å, respectively. The O−C−O angle is 127.5(7)°.

Table 3. Relevant Bond Lengths (Å) and Angles (deg) for $[Ba_2(O_2CCF_3)_4(tetraglyme)]_\infty$ (**2**)

Bond Distances			
Ba−O1	3.080(5)	Ba−O2	2.802(S)
Ba−O3	2.780(5)	Ba−O4	2.953(5)
Ba−O5	2.854(5)	Ba···Ba[a]	4.316(1)
Ba−O6	2.680(6)	Ba−O4a	2.773(4)
Ba···Ba[b]	4.508(1)	Ba−O7a	2.667(6)
Ba−O5b	2.743(4)		
Bond Angles			
O4−Ba−O5	44.5(1)	O4−Ba−O6	74.5(2)
O4−Ba−O4a	82.3(2)	O5−Ba−O6	84.1(2)
O5−Ba−O5b	67.3(2)	O5−Ba−O4a	126.5(1)
O6−Ba−O5b	88.3(2)	O6−Ba−O4a	74.8(2)
O5−Ba−O7a	94.4(2)	O4−Ba−O5b	110.4(1)
O6−Ba−O7a	134.O(2)	O4a−Ba−O5b	155.6(2)
O5a−Ba−O7a	133.3(2)	O4−Ba−O7a	72.8(2)
Ba−O4−Ba[a]	97.7(2)	O4a−Ba−O7a	69.6(2)
Ba−O1−Ba[b]	94.1(2)	Ba−O5−Ba[b]	107.3(2)
O6−C8−O7	132.0(8)	O4−C6−O5	127.5(7)

These values are intermediate between those associated with purely bridging or chelating carboxylates. As one might expect, the purely bridging trifluoroacetate ligand of $[Ba_2(O_2CCF_3)_4$-(tetraglyme)$]_\infty$ has an average $Ba-O_{carboxylate}$ and O−C−O angle quite close to those observed for the bridging trifluoroacetate ligands of $Ba_2(O_2CCF_3)_4(15\text{-crown-}5)_2$ (2.674[9] vs 2.644[12] Å and 132.0(8) vs 131.3(13)°, respectively). The chelating and bridging oxygen atoms of the tetraglyme ligand have $Ba-O_{ether}$ bond distances of 2.791[16] and 3.080(5) Å, respectively. Although the Ba−O bond is shorter for bridging vs chelating carboxylate ligands, the reverse relationship is operative for the bridging and chelating oxygen atoms of the tetraglyme ether.

Comparison of IR data of a number of $Ba(O_2CCF_3)_2L$ compounds including $Ba_2(O_2CCF_3)_4(15\text{-crown-}5)_2$ and $[Ba_2$-$(O_2CCF_3)_4(tetraglyme)]_\infty$ (see Experimental Section) suggests that purely bridging carboxylates have $\nu_{asym}(CO_2)$ stretching frequencies above those that are either chelating or both bridging and chelating.[20] However, the frequency of $\nu_{asym}(CO_2)$ has been found to be quite dependent on the number and type of donating atoms of the neutral polydentate ligand. For example, in the isostructural series $Ba_2(O_2CCF_3)_4(polyether)_2$, where polyether = 15-crown-5, 12-crown-4, or triglyme, the $\nu_{asym}(CO_2)$ for the bridging carboxylate of the 12-crown-4 and triglyme compounds are similar (1690 and 1693 cm^{-1}, respectively), whereas the

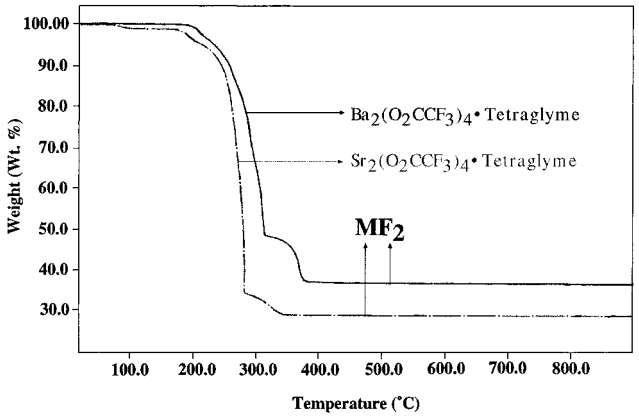

Figure 3. TGA data for the compounds $[M_2(O_2CCF_3)_4(\text{tetraglyme})]_\infty$, where M = Ba and Sr.

15-crown-5 compound has a value of 1717 cm^{-1}. The additional donating oxygen atom of the 15-crown-5 polyether appears to increase the $\nu_{asym}(CO_2)$ frequency by about 30 cm^{-1}. This may be the result of increased electron density at the metal center provided by the polyether ligand which would tend to increase the CO bond order in the bridging carboxylate ligand.

The similarity in the IR and NMR spectra and thermal decomposition (*vide infra*) of $[Sr_2(O_2CCF_3)_4(\text{tetraglyme})]_\infty$ (**3**) with that of $[Ba_2(O_2CCF_3)_4(\text{tetraglyme})]_\infty$ (**2**) suggests that these two compounds are structurally similar. The presence of only 0.5 tetraglyme ligands per strontium center as indicated by elemental analysis is consistent with the elemental analysis result obtained for the barium compound.

The thermal behavior of $Ba_2(O_2CCF_3)_4$(15-crown-5)$_2$ and $[M_2(O_2CCF_3)_4(\text{tetraglyme})]_\infty$ (M = Sr, Ba) was investigated by thermogravimetric analysis (TGA) in air. The TGA of $Ba_2(O_2CCF_3)_4$(15-crown-5)$_2$ exhibited a single weight loss at 280 °C with formation of BaF_2 as confirmed by powder X-ray diffraction while $[M_2(O_2CCF_3)_4(\text{tetraglyme})]_\infty$ thermally decomposed to form MF_2 by 350 °C (M = Sr) and 380 °C (M = Ba) as shown in Figure 3. These data suggest that, through a pure thermal decomposition mechanism, these barium carboxylate compounds are unlikely to be a viable source of Ba in formation of $BaTiO_3$ materials at low temperatures since it has been shown that formation of intermediate phases such as $BaCO_3$ or BaF_2 is detrimental to $BaTiO_3$ formation.[23,24] However, if the carboxylate ligands can be eliminated by an alternative reaction such as ester elimination prior to their thermal decomposition, this problem may be alleviated.

The reaction of these polyether barium carboxylate compounds with Ti(O-*i*-Pr)$_4$ was studied by spin coating ethanol solutions of these species onto Si and Pt/Si substrates followed by thermal treatments to different temperatures. X-ray diffraction data of films prepared from $Ba_2(O_2CCF_3)_4$(15-crown-5)$_2$ on Pt/Si substrates showed only the presence of crystalline BaF_2 at 350 and 450 °C and a mixture of crystalline $BaTiO_3$ and BaF_2 at 550 and 650 °C. The analysis of films by Auger electron spectroscopy (AES) gives information on the film composition including amorphous material as well as the level of impurities. The Auger data for films prepared from $Ba_2(O_2CCF_3)_4$(15-crown-5)$_2$ showed the presence of about 12 and 14 atomic % carbon in the films prepared at 350 and 650 °C, respectively. The amount of fluorine in the film at 650 °C is much lower than in film deposited at 350 °C, but is still around 4 atomic % F. The fluorine in the film at 650 °C appears to be

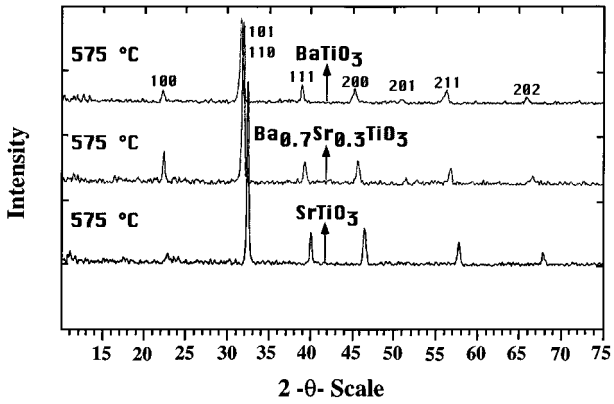

Figure 4. Powder X-ray diffraction patterns for $MTiO_3$ (M = Sr, Ba, $Ba_{0.7}Sr_{0.3}$) films derived from the reaction between $[M_2(O_2CCF_3)_4(\text{tetraglyme})]_\infty$ and Ti(O-*i*-Pr)$_4$ after heating to 575 °C.

Table 4. Elemental Composition of the Films Derived from Compounds **2** and **3** As Determined by Auger Electron Spectroscopy after 6 min Sputtering

sample (anneal temp)	Sr	Ba	Ti	O	F	C
$SrTiO_3$ (tetraglyme)[a] (350 °C)	0.18		0.20	0.46	0.12	0.04
$SrTiO_3$ (tetraglyme)[b] (575 °C)	0.19		0.19	0.55		0.07
$BaTiO_3$ (tetraglyme)[a] (350 °C)		0.15	0.19	0.48	0.09	0.08
$BaTiO_3$ (tetraglyme)[b] (575 °C)		0.15	0.20	0.60		0.05
Ba(Sr)TiO_3 (tetraglyme)[a] (350 °C)	0.07	0.09	0.19	0.54	0.12	0.11
Ba(Sr)TiO_3 (tetraglyme)[b] (575 °C)	0.05	0.10	0.20	0.60		0.05

[a] Amorphous by glancing angle X-ray diffraction. [b] Crystalline by glancing angle X-ray diffraction.

in the form of MF_2 by X-ray diffraction. When a film prepared from $Ba_2(O_2CCF_3)_4$(15-crown-5)$_2$ and Ti(OvsPr)$_4$ and annealed at 350 °C is then annealed at 550 or 650 °C for 4 h, a crystalline perovskite $BaTiO_3$ phase grows in. Where at 350 °C only BaF_2 is observed as the crystalline phase, both BaF_2 and $BaTiO_3$ are observed at 550 or 650 °C. From these data, it would appear that the $BaTiO_3$ may be present in the film at 350 °C in amorphous form but does not crystallize until 550 °C or above.

In contrast, X-ray diffraction of films deposited from solutions of $[M_2(O_2CCF_3)_4(\text{tetraglyme})]_\infty$ and Ti(i-OPr)$_4$ showed that amorphous films were formed in the temperature range 350−500 °C and crystalline $MTiO_3$ (M = Sr, Ba, $Ba_{0.7}Sr_{0.3}$) at 575 °C and above with no evidence for crystalline metal fluorides as shown in Figure 4. Auger electron spectroscopy of the amorphous films deposited at 350 °C showed some fluorine contamination but these films upon annealing at 575 °C exhibited no detectable fluorine content; see Table 4. The amount of oxygen in the films appears to increase as the fluorine level falls below the instrumental detection limit (1.0 atomic %) for the films annealed at 575 °C and the amount of C contamination drops. The chemical form of the fluorine in the amorphous films is unclear, however, it is probably not MF_2 which should be crystalline at 350 °C (see above, $Ba_2(O_2CCF_3)_4$-(15-crown-5)$_2$ films) and detected by X-ray diffraction. The Sr:Ti:O ratio in both the amorphous and crystalline films had an elemental composition by AES consistent with the expected ratio in the film. The concentration of Ba in the Ba-containing films was always lower than that for the stoichiometry of the compound expected (Table 4) but this observation can be explained as a result of preferential sputtering of Ba during Ar^+ ion sputtering of the film. This was investigated in a series of control experiments in which authentic samples of stoichiometric $BaTiO_3$ powders were sputtered under analogous conditions, and it was found that this effect is difficult to predict.

It is interesting to note that the lower fluoride content of films derived from the tetraglyme compounds compared to the 15-

(23) Grammatico, J. P.; Porto Lopez, J. M. *J. Mater. Sci.: Mater. Electron.* **1992**, *3*, 82.
(24) Datta, G.; Maiti, H. S.; Paul, A. *J. Mater. Sci. Lett.* **1987**, *6*, 787.

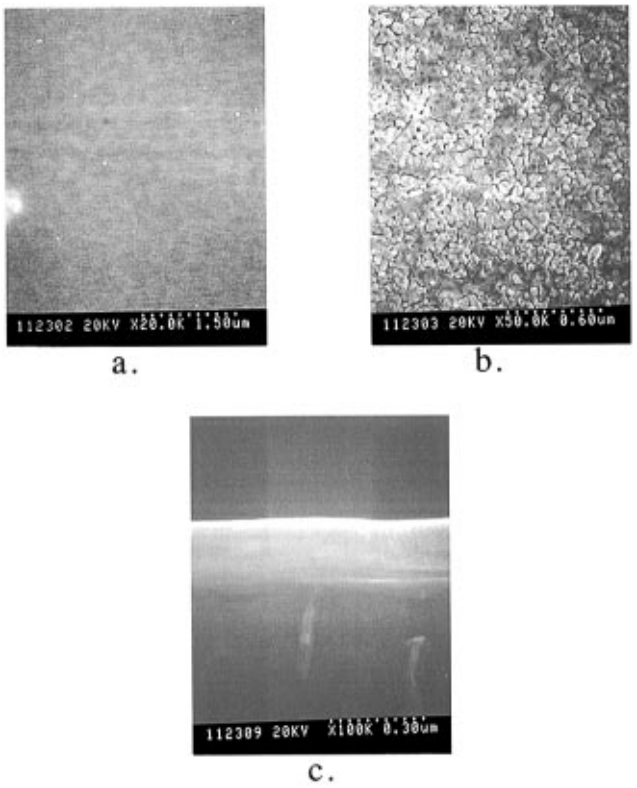

Figure 5. (a,b) SEM data for a $BaTiO_3$ film derived from the reaction between $[M_2(O_2CCF_3)_4(tetraglyme)]_\infty$ and $Ti(O\text{-}i\text{-}Pr)_4$ after heating to (a) 350 °C or (b) 575 °C. (c) Cross section of the film annealed at 575 °C.

crown-5 compounds. This is a valuable observation in the sense that, because all the processing conditions were identical, the difference in the composition of the film is derived from the nature of these compounds. The difference in reactivity could be derived from the difference in coordination mode of the carboxylate ligands or the binding of the polyether ligand.

The morphology of the films is represented by the micrographs shown in Figure 5 which show top views and a cross section of the $BaTiO_3$ films. The film appears fairly dense in cross section but it is clear that there are voids between regions of fused crystallites based on the top view.

It is apparent from these results that there is a considerable difference in the thermal reactivity of these Sr and Ba carboxylate compounds in the presence and absence of $Ti(O\text{-}i\text{-}Pr)_4$. If the alkoxide and fluoroacetate ligands reacted via ester elimination, we would expect the amount of fluorine and carbon in the films to be significantly lower than is the case for independent thermal decomposition of the group 2 or Ti compounds. A series of experiments were carried out to determine if esters were formed during this reaction. No reaction appears to occur between $[Ba_2(O_2CCF_3)_4(tetraglyme)]_\infty$ and $Ti(O\text{-}i\text{-}Pr)_4$, Ba:Ti (1:1), in THF at room temperature with the $[Ba_2(O_2CCF_3)_4(tetraglyme)]_\infty$ recoverable from solution unchanged. A mixture of $[Ba_2(O_2CCF_3)_4(tetraglyme)]_\infty$ and $Ti(O\text{-}i\text{-}Pr)_4$, 1:1 (Ba:Ti), was heated in toluene to 110 °C in a sealed NMR tube for 4 days. Again, no reaction was observed, and we concluded that a higher temperature for reaction was required. A mixture of $[Ba_2(O_2CCF_3)_4(tetraglyme)]_\infty$ and excess $Ti(O\text{-}i\text{-}Pr)_4$ was heated in a sealed ampule for 1 day at 250 °C. Under these conditions a reaction occurred and a brown solid formed; however, this product and the volatile byproducts could not be unambiguously identified by NMR and it is likely they represent a mixture of thermal decomposition products of the initial reaction byproducts. Attempts to identify the volatile byproducts evolved from the reaction between $[Ba_2(O_2CCF_3)_4(tetraglyme)]_\infty$ and an excess of $Ti(O\text{-}i\text{-}Pr)_4$ by TGA/mass spectroscopy (MS) were also unfruitful due to the low concentration of products evolved and the dominating effect of the O-*i*-Pr fragments.

Compounds **1**−**3** decompose rather than sublime when heating under reduced pressure (10^{-2} Torr). Free crown and metal carboxylate are the primary products as determined by NMR spectroscopy. This makes these compounds unsuitable for conventional chemical vapor deposition. However, their employment as useful precursors for the formation of $MTiO_3$ films by aerosol assisted chemical vapor deposition, where low volatility can be tolerated, is under investigation.

Conclusions

As a result of these observations, we conclude that these barium carboxylate compounds are suitable precursors for the formation of $BaTiO_3$ films by liquid phase routes at low temperatures provided that thermal decomposition of the carboxylate ligand to form BaF_2 can be avoided. The observation that the barium compounds thermally decompose to deposit metal fluoride films in the absence of $Ti(O\text{-}i\text{-}Pr)_4$, while the fluorine content is significantly lower in the presence of $Ti(O\text{-}i\text{-}Pr)_4$ is consistent with the presence of a reaction mechanism which results in elimination of the fluorinated carboxylate ligand prior to its thermal decomposition. Attempts to study the byproduct evolution during film deposition have been unsuccessful due to the small amount of byproducts evolved. Further studies are in progress to understand the reaction chemistry and phase evolution in these systems.

Acknowledgment. We thank Texas Instruments and the AFOSR for financial support of this work, the NSF chemical instrumentation program for the purchase of a low-field NMR spectrometer, and AFOSR and the Dreyfus Foundation for the purchase of a powder X-ray diffractometer. M.H.S. thanks Ms. Nena Davis for technical assistance.

Supporting Information Available: Tables of crystal data, positional parameters and equivalent isotropic displacement coefficients, bond distances and angles and anisotropic displacement coefficients, and a refinement summary for **1** and **2** (30 pages). Ordering information is given on any current masthead page.

IC960660Y